ELSEVIER

J. Non-Newtonian Fluid Mech. 93 (2000) 325–337

Journal of Non-Newtonian Fluid Mechanics

www.elsevier.com/locate/jnnfm

Axial annular flow of a nonlinear viscoelastic fluid — an analytical solution

Fernando T. Pinho [a], Paulo J. Oliveira [b,*]

[a] *Centro de Estudo de Fenómenos de Transporte, DEMEGI, Faculdade de Engenharia da Universidade do Porto, Rua dos Bragas, 4050-123 Porto, Portugal*

[b] *Departamento Eng Electromecânica, Universidade da Beira Interior, 6200 Covilhã, Portugal*

Received 25 January 2000; received in revised form 2 March 2000

Abstract

An analytical solution is given for the kinematic and stress variations across the radial gap of a concentric annular flow in fully developed conditions. The fluid is viscoelastic and obeys the non-linear rheological constitutive equation proposed by Phan-Thien and Tanner [1]. This constitutive model simulates well the material functions of many polymer melts and solutions and therefore, the present results are useful in a number of practical situations. The ratio of pressure drop to flow rate drop is found to be a complex mathematical function of the radial position of zero shear stress and this, in turn, depends weakly on the elasticity, based on the product of an elongational parameter by a Deborah number defined with an averaged velocity. There is thus a non-linear coupling which could not be solved in an explicit way for the inverse problem of an imposed flow rate, but an iterative procedure gives a ready result. For the direct problem of a given pressure drop the present results represent an exact explicit solution to the axial annular flow problem. Representative profiles of the solution are given and discussed. It is found that, for a given flow rate, the pressure drop scaled with the corresponding Newtonian value is independent of the diameter ratio.

Keywords: Annular flow; Analytical solution; Viscoelastic fluid; Phan-Thien–Tanner Model fluid

1. Introduction

Laminar annular flows of viscous fluids are frequently encountered in industry, two examples being annular heat exchangers in the food industry and drilling operations. In both cases the fluids, either synthetic or natural, are mixtures of different stuffs such as water, particles, oils and other long chain molecules; this combination imparts strong non-Newtonian characteristics to the resulting liquids: the viscosity function varies non-linearly with the shear rate; elasticity is felt through first-normal stress and

* Corresponding author. Fax: +351-275-320820.
E-mail addresses: fpinho@fe.up.pt (F.T. Pinho), pjpo@ubi.pt (P.J. Oliveira)

0377-0257/00/$ – see front matter
PII: S0377-0257(00)00113-0

elongational effects; and time-dependent effects such as thixotropy may also be present (Kokini et al. [2]; Alderman et al. [3]). In drilling applications, if the additional complications arising from rotation of the inner cylinder and possible eccentricity of the annulus are removed, one ends up with the problem of knowing the kinematic and stress fields in the axial flow of a viscoelastic fluid through a concentric annular gap.

For the simple case of a Newtonian fluid, the exact solution to the problem of axial annular flow can be found in classical textbooks (see e.g. Bird et al. [4], pp. 51–54). For power law, inelastic, non-Newtonian fluids the problem was first studied by Fredrickson and Bird [5] who presented a relation between the flow rate and the pressure gradient in terms of an integral which required numerical quadrature. This was rather cumbersome to use in practical calculations and Hanks and Larsen [6] were later able to derive a simpler analytical solution to the flow rate/pressure drop relation. However, even for this case, one of the integration constants representing the radial position of nil shear stress, was the solution of an integral equation which could not be evaluated explicitly and was only given in tabulated form. Hanks [7] also studied the case of the viscoplastic Herschel–Bulkley model and gave design charts for the computation of the flow rate in terms of pressure drop, or vice versa. References to other studies with different inelastic rheological models can be found in this latter work, and some of those are discussed in the excellent book by Bird, Armstrong and Hassager [8] (pages 221 (Ellis fluid), 226 (helical flow of power-law fluid), 230 and 265 (power-law fluid), 267 (Bingham fluid)).

Literature is scarcer on annular flow of viscoelastic fluids. Experimental measurements of concentrated CMC solutions have been reported by Nouar et al. [9] and Naimi et al. [10], but these results can be fairly predicted by assuming a pure viscous behaviour (Escudier et al. [11]). Theoretical/numerical work with simplified viscoelastic fluid models are less frequent; two works of that type are those of Savins and Wallick [12] and Dierckes and Schowalter [13] with linear models. An extensive literature survey in preparation by Escudier et al. [11] has shown that there appears to be no published solutions for the same problem with elastic fluids obeying non-linear differential equations for the evolution of the stress tensor.

In the present work, we selected one of the most often used non-linear viscoelastic model fluids and derived analytical expressions for the velocity and stress (shear and normal components) profiles in concentric annular flow. The solution includes relations between the normalised pressure drop and flow rate (friction factor and Reynolds number) as a function of the relevant dimensionless parameters (Reynolds number, Deborah number and elongational parameter in the rheological model). For the 'direct' problem in which the pressure drop is given and the flow rate is unknown, the present solution is a fully explicit exact solution. For the more useful 'inverse' problem, in which the flux is known and the pressure drop unknown, a coupling between two cubic equations does not allow an explicit analytical solution but simple iteration between those two equations allows a solution to be obtained without difficulty, as will be shown.

The model fluid considered in this analysis is that governed by the simplified Phan-Thien and Tanner [1] constitutive equation (hereafter denoted by PTT):

$$\left(1 + \frac{\epsilon\lambda}{\eta}\mathrm{tr}(\tau)\right)\tau + \lambda\overset{\nabla}{\tau} = 2\eta D, \tag{1}$$

where τ and D are the extra-stress and deformation-rate tensors, λ the relaxation time, η the constant viscosity coefficient and $\overset{\nabla}{\tau}$ denotes Oldroyd's upper convected derivative,

$$\overset{\nabla}{\tau} = \frac{Du}{Dt} - \tau\cdot\nabla u - \nabla u^t\cdot\tau.$$

The parameter ϵ in Eq. (1) is related to the elongational behaviour of the fluid, precluding the possibility of an infinite elongational viscosity in a simple stretching flow as would occur for an upper Maxwell model UCM, in which $\epsilon=0$.

The PTT model has found widespread use in numerical simulations of the flow of polymer solutions and melts. It has been found by Quinzani et al. [14] to be an excellent simple differential model for the elongational properties of polymer solutions in entry flows. Even more relevant is the fact that it can also predict accurately the shear properties of those same fluids, and these features make it adequate for use in predominantly viscometric flows, as the one considered here (Peters et al. [15]). Many authors have also used the PTT model in numerical studies of contraction and expansion flows, of which we mention White and Baird [16], Baaijens [17], Carew et al. [18], Azaiez et al. [19], Baloch et al. [20], to give only a few examples, and this same model has been used in many other types of flows. This widespread interest on the PTT model gives support for the usefulness of the present study.

2. Analysis

The problem under consideration is that of fully developed axial flow with cylindrical symmetry in the annular gap between two concentric cylinders, with inner and outer radius given, respectively, by R_i and R_o ($\delta \equiv R_\mathrm{o}-R_\mathrm{i}$) The axial velocity component, along coordinate z, is denoted u and it is only a function of the radial coordinate r. There are four non-dimensional parameters to this flow problem: the radius ratio $k=R_\mathrm{i}/R_\mathrm{o}$ (geometric parameter); the Reynolds number $\mathrm{Re}=\rho U 2\delta/\eta$ (dynamic parameter); ϵ and the Deborah number $\mathrm{De}=\lambda U/\delta$ (constitutive parameters). It is standard practice to base the Reynolds number on the hydraulic diameter $D_\mathrm{H}=4A/P$, where A is the cross-section area and P the wetted perimeter, which for an annulus gives $D_\mathrm{H}=2\delta$.

2.1. Stress relations

For the particular case here considered of unidirectional flow in cylindrical coordinates the axial momentum equation reduces to

$$\frac{1}{r}\frac{\mathrm{d}}{\mathrm{d}r}(r\tau_{rz}) = p_{,z}, \tag{2}$$

where $p_{,z}\equiv \mathrm{d}p/\mathrm{d}z$ is the constant pressure gradient and τ_{rz} the shear stress component. Upon integration this equation gives

$$\tau_{rz} = -p_{,z}\frac{R_*}{2}\left(\frac{R_*}{r}-\frac{r}{R_*}\right), \tag{3}$$

where the natural boundary condition of no-slip at the inner cylinder ($u=0$ at $r=R_\mathrm{i}$) has been replaced, following Fredrickson and Bird [5] and Bird at al. [4] (p. 52), by a zero shear stress condition: $\tau_{rz}=0$ at $r=R_*$. The development of the foregoing analysis gives rise to a characteristic velocity scale defined by

$$U_\mathrm{c} = \frac{-p_{,z}\delta^2}{8\eta}, \tag{4}$$

with which we have implicitly associated a length scale, chosen as the annulus gap δ. This choice for length scale is also implicit in the above definitions for the Reynolds and Deborah numbers. Other velocity scales could be defined if the length scale had been chosen as the outer cylinder radius (as in the works of Bird et al.), or the inner radius. These choices are less advantageous when the limit for either simple pipe flow ($R_\mathrm{i} \to 0$) or channel flow ($\delta/R_\mathrm{i} \to 0$) are sought. On the other hand, the various expressions resulting from the present non-dimensionalisation can be easily changed to the other forms if need be. With the present non-dimensional choice the radial coordinate is denoted $y \equiv r/\delta$ and the shear stress becomes

$$T_{rz} \equiv \frac{\tau_{rz}}{\eta(U/\delta)} = 4y_* \frac{U_\mathrm{c}}{U}\left(\frac{y_*}{y} - \frac{y}{y_*}\right), \tag{5}$$

where $y_* \equiv R_*/\delta$ and U is the average velocity in the annulus. This average velocity is usually a given quantity, defined as the volumetric flow rate divided by the cross sectional area ($U \equiv Q/\pi(R_\mathrm{o}^2 - R_\mathrm{i}^2)$) and can be related to the pressure gradient once the velocity variation is known, as will be shown below.

The constitutive equation for the only two non-vanishing stress components, from Eq. (1), give

$$\tau_{rz} = \frac{\eta}{1 + (\epsilon\lambda/\eta)\tau_{zz}}\dot{\gamma}, \tag{6}$$

$$\tau_{zz} = \frac{2\lambda\eta}{(1 + (\epsilon\lambda/\eta)\tau_{zz})^2}\dot{\gamma}^2, \tag{7}$$

where $\dot{\gamma} \equiv \mathrm{d}u/\mathrm{d}r$ is the velocity gradient and the trace of the stress tensor reduces to τ_{zz}. If Eq. (7) is divided by the square of Eq. (6) then the following relationship between stress components is obtained:

$$\tau_{zz} = \frac{2\lambda}{\eta}\tau_{rz}^2. \tag{8}$$

With the above definition for the Deborah number, the axial normal stress component is written in non-dimensional form as

$$T_{zz} = 2\,\mathrm{De}\,T_{rz}^2. \tag{9}$$

At this point there are two relations for the variation of stress components across the annulus, Eq. (5) for T_{rz} and Eq. (9) for T_{zz}, as well as a third equation relating the stresses and the velocity gradient, Eq. (6).

2.2. Kinematic relations

The velocity gradient is made explicit from Eq. (6) to give

$$\dot{\gamma} = \frac{1}{\eta}\tau_{rz}\left(1 + \frac{\epsilon\lambda}{\eta}\tau_{zz}\right),$$

and can be normalised using the definition $\Gamma \equiv \dot{\gamma}/(U/\delta)$ into

$$\Gamma = T_{rz}(1 + \epsilon\,\mathrm{De}\,T_{zz}). \tag{10}$$

Upon substitution of Eqs. (5) and (9) into Eq. (10) we obtain an explicit equation for the velocity gradient in terms of the normalised radial coordinate

$$\frac{\mathrm{d}v}{\mathrm{d}y} = 4y_* \frac{U_\mathrm{c}}{U}\left(\frac{y_*}{y} - \frac{y}{y_*}\right)\left(1 + 2\epsilon\,\mathrm{De}^2\left(4y_*\frac{U_\mathrm{c}}{U}\left(\frac{y_*}{y} - \frac{y}{y_*}\right)\right)^2\right), \tag{11}$$

with $v \equiv u/U$ denoting the non-dimensional axial velocity component. Eq. (11) can be integrated to give

$$\begin{aligned} v \equiv \frac{u}{U} = 4Xy_*^2 \Bigg[& \left\{ \ln\frac{y(1-k)}{k} - \frac{y^2 - (k/(1-k))^2}{2y_*^2} \right\} \\ & -32\epsilon\,\mathrm{De}_\mathrm{c}^2 y_*^2 \left\{ 3\ln\frac{y(1-k)}{k} + \frac{y^2 - (k/(1-k))^2}{2y_*^2}\left(\frac{y^2 + (k/(1-k))^2}{2y_*^2} - 3\right) \right. \\ & \left. + \frac{y_*^2}{2}\left(\frac{1}{y^2} - \frac{(1-k)^2}{k^2}\right) \right\} \Bigg], \end{aligned} \tag{12}$$

where $\mathrm{De}_\mathrm{c} \equiv \lambda U_\mathrm{c}/\delta$ is a new Deborah number based on the velocity scale U_c which can be related to the usual definition by $\mathrm{De}_\mathrm{c} = \mathrm{De}\,X$. Here $X \equiv U_\mathrm{c}/U$ is an unknown of the problem to be found later and has the physical meaning of a non-dimensional pressure gradient. To arrive at Eq. (12) it was necessary to use the no-slip condition at the inner cylinder surface ($u=0$ at $y = R_\mathrm{i}/\delta = k/(k-1)$).

2.3. Solution for $y_* = R_*/\delta$

As mentioned above and following Fredrickson and Bird [5], the no-slip condition at the inner surface was replaced by the condition $\tau_{rz}=0$ at $y = y_* \equiv R_*/\delta$ which is satisfied identically by the shear stress Eq. (5), and so y_* still remains to be determined. The second boundary condition expresses no-slip at the outer cylinder and can be written with the normalised variables as

$$v = 0 \;\text{ at }\; y = \frac{1}{1-k}.$$

If we insert it into Eq. (12) and proceed to regroup the various terms in powers of y^* we end up with a cubic equation for $x \equiv y_*^2$:

$$x^3 + a_1 x^2 + a_2 x + a_3 = 0, \tag{13}$$

where

$$a_1 = \frac{6\ln k}{(1-k^2)((1/k)-1)^2}, \tag{14}$$

$$a_2 = \frac{3k^2}{(1-k)^4} - \frac{2\ln k}{(32\epsilon\,\mathrm{De}_\mathrm{c}^2)(1-k)^2((1/k)^2-1)},$$

$$a_3 = -\frac{k^2}{(1-k)^4}\left(\frac{1}{32\epsilon\,\mathrm{De}_\mathrm{c}^2} + \frac{1+k^2}{2(1-k)^2}\right).$$

For a fluid with infinite extensibility or devoid of elasticity we have $\epsilon=0$ or $\lambda=0$ the velocity profile of Eq. (12) retains only the first term on the right-hand-side, and the null shear stress radial position reduces to

$$y_* \equiv (y_*)_{\mathrm{N}} = \left(\frac{1+k}{2(1-k)\ln(1/k)}\right)^{1/2}, \tag{15}$$

that is, $R_*^2 = -(R_0^2 - R_\mathrm{i}^2)/2\ln(k)$, the value given by Bird et al. [4] (p. 52) for the Newtonian case. We use the index 'N' to denote the Newtonian case but it should be emphasised that the above result is also valid for a purely elastic fluid ($\epsilon=0$). The real solution to the cubic Eq. (13) can be determined explicitly by the formulae for third order algebraic equations

$$x = \mathrm{sign}(p)|p|^{1/3} + \mathrm{sign}(q)|q|^{1/3} - \frac{a_1}{3}, \tag{16}$$

with

$$p = -\frac{b}{2} + d^{1/2}, \tag{17}$$

$$q = -\frac{b}{2} - d^{1/2},$$

$$d = \frac{b^2}{4} + \frac{a^3}{27},$$

$$a = a_2 - \frac{a_1^2}{3},$$

$$b = a_3 - \frac{a_1 a_2}{3} + \frac{2a_1^2}{27}.$$

Now, the coefficients a_2 and a_3 depend on $\mathrm{De_c}$, and thus on $X=U_\mathrm{c}/U$, which can be determined only after the velocity profile is known, following the procedure explained hereafter.

2.4. The average velocity: solution for $X=U_\mathrm{c}/U$

From its definition, the cross-section average velocity is given by

$$U = \frac{1}{(R_\mathrm{o}^2 - R_\mathrm{i}^2)\pi}\int_{R_\mathrm{i}}^{R_\mathrm{o}} u(r)2\pi r\,\mathrm{d}r, \tag{18}$$

or, in terms of non-dimensional coordinates,

$$U = \frac{2(1-k)}{(1+k)}\int_{k/(1-k)}^{1/(1-k)} u(y)y\,\mathrm{d}y. \tag{19}$$

If the velocity variation from Eq. (12) is substituted for $u(y)$ above and the integration is performed, the following equation is obtained for $X=U_\mathrm{c}/U$:

$$\frac{1}{y_*^2(8(1-k)/(1+k))} = I_1 X - 32\epsilon\,\mathrm{De}^2 y_*^2 I_2 X^3, \tag{20}$$

with

$$I_1 = \int_{k/(1-k)}^{1/(1-k)} \left(\ln\frac{y(1-k)}{k} - \frac{y^2 - (k/(1-k))^2}{2y_*^2} \right) y \, \mathrm{d}y$$
$$= \frac{\ln(1/k)}{2(k-1)^2} + \frac{(k+1)(2y_*^2(k-1) - k - 1)}{8y_*^2(k-1)^2} \tag{21}$$

and

$$I_2 = \int_{k/(1-k)}^{1/(1-k)} \left[3\ln\frac{y(1-k)}{k} + \frac{y^2 - (k/(1-k))^2}{2y_*^2} \left\{ \frac{y^2 + (k/(1-k))^2}{2y_*^2} - 3 \right\} \right.$$
$$\left. + \frac{y_*^2}{2} \left\{ \frac{1}{y^2} - \frac{(1-k)^2}{k^2} \right\} \right] y \, \mathrm{d}y = \left(\frac{y_*^2}{2} + \frac{3}{2(k-1)^2} \right) \ln\frac{1}{k}$$
$$+ \frac{(1+k)(6y_*^6(k-1)^5 + 18y_*^4k^2(k-1)^3 - 9y_*^2k^2(k-1)^2(k+1) + k^2(k+1)(2k^2+1))}{24y_*^4k^2(k-1)^4}. \tag{22}$$

The real solution to the cubic Eq. (20) is

$$X = \frac{432^{1/6}(D^{2/3} - 2^{2/3}\alpha)}{6\beta^{1/2}D^{1/3}}, \tag{23}$$

with

$$\alpha = I_1 y_*^2 \left(\frac{8(1-k)}{1+k} \right),$$
$$\beta = -32\epsilon \, \mathrm{De}^2 y_*^4 I_2 \left(\frac{8(1-k)}{1+k} \right),$$
$$D = (4\alpha^3 + 27\beta)^{1/2} + 3^{3/2}\beta^{1/2}.$$

Hence we see that X (Eq. (20)) depends on $y_*^2 \equiv x$, which itself (Eq. (13)) depends on X through $\mathrm{De_c}=\mathrm{De}\,X$. Therefore, an iterative procedure will be required to resolve this non-linear coupling. As it will be shown, x is not too different from x_N (the corresponding value for Newtonian fluids) and a few iterations on the above solution equations for x and X, starting with $x=x_\mathrm{N}$, are sufficient to have values for x and X accurate to a very tight tolerance.

2.5. Friction factor

One important engineering parameter is the Fanning friction factor

$$f \equiv \frac{\Delta p}{4(L/D_\mathrm{H})(\rho U^2/2)} = \frac{-p_{,z}D_\mathrm{H}}{2\rho U^2}, \tag{24}$$

and in Newtonian flow the factor $f\mathrm{Re}$ is a function of the radius ratio only (see Bird et al. [4], p. 53):

$$(f\,\mathrm{Re})_\mathrm{N} = 16\frac{1}{(1+k^2)/(1-k)^2 - (1+k)/(1-k)(1/\ln(1/k))}. \tag{25}$$

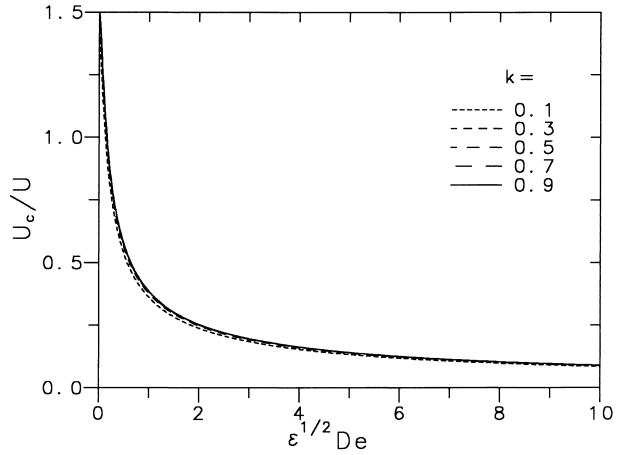

Fig. 1. Solution to Eq. (20) written in terms of U_c/U vs. $\epsilon^{1/2}$ De for various diameter ratios $k(U_c \equiv -p_z\delta^2/8\eta;\ \ \mathrm{De} \equiv \lambda U/\delta)$.

In the case of the present PTT fluid the factor $f\,\mathrm{Re}$ is obtained directly from its definition (24):

$$f\,\mathrm{Re} = 16\frac{U_c}{U} \tag{26}$$

and $U_c/U \equiv X$ is calculated from Eq. (23). It is remarked that the close analogy of $f\,\mathrm{Re}$ from Eq. (26) for the PTT fluid in the annular gap and the well-known result for Newtonian fluid, $f\,\mathrm{Re}=16$, is a consequence of the adopted velocity scale, as defined by Eq. (4).

3. Results

Fig. 1 gives the ratio between the pressure drop and the average velocity (U_c/U) as a function of the group $\epsilon^{1/2}$ De, which characterises the elasticity and extensibility of the fluid, for various values of the

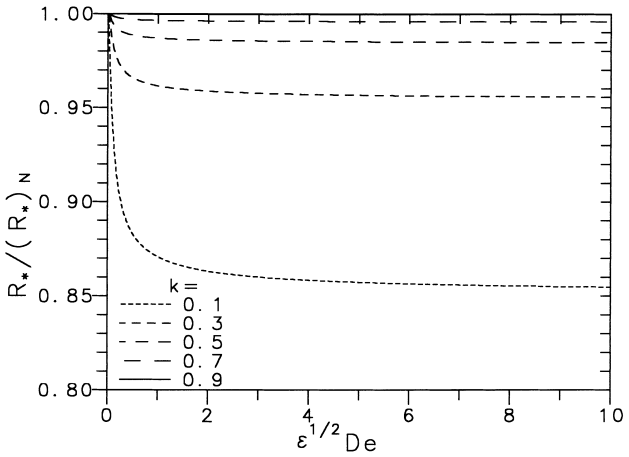

Fig. 2. Radial position of the zero-shear stress point (R_*) scaled with corresponding Newtonian value ($(R_*)_N$) vs. $\epsilon^{1/2}$ De for various diameter ratios.

Table 1
Number of iterations to solve Eqs. (13) and (20) and their solution

ϵ	De	k	Iteration (tol 10^{-5})	y_*	X
0.25	0.1	0.2	6	0.6740	1.3153
0.25	0.1	0.5	4	1.4679	1.3630
0.25	0.1	0.8	3	4.4897	1.3739
0.25	1.0	0.2	7	0.6419	0.5554
0.25	1.0	0.5	5	1.4541	0.5726
0.25	1.0	0.8	4	4.4853	0.5767
0.25	5.0	0.2	5	0.6332	0.2127
0.25	5.0	0.5	4	1.4500	0.2186
0.25	5.0	0.8	4	4.4840	0.2200

annulus ratio k. This is thus the solution given by Eq. (23) to the second cubic Eq. (20); the curves for the various radius ratios k almost collapse (although not quite for small $\epsilon^{1/2}$ De). As seen in the figure, with increased k and $\epsilon^{1/2}$ De the scaled pressure gradient required to drive a given flow rate is reduced. At vanishing elasticity, the proper limits of $U_c/U=1.5$ for high k ($k=1$, for a plane channel) and $U_c/U=1$ for low k ($k=0$, for a pipe) are recovered, although this latter limit requires much lower values of k than the 0.1 shown in the figure.

Fig. 2 shows the zero-shear stress position (R_*), normalised with the corresponding Newtonian value $\left((R_*)_N = \left((R_o^2 - R_i^2)/2\ln(1/k)\right)^{1/2}\right)$ as a function of the elasticity parameter $\epsilon^{1/2}$ De, for various values of k. These values correspond to the solution of the cubic Eq. (13) which is coupled with Eq. (20), as discussed above. For $k \geq 0.3$, R_* is only marginally different from the Newtonian value (differences below 4%) and is independent of the elasticity for $\epsilon^{1/2}$ De ≥ 0.5. For smaller radius ratios, for example for $k=0.1$, the differences are about 14% at high De. It is remarked that $y_*=R_*/\delta$ is not independent of k, as was approximately the case with the scaled pressure gradient.

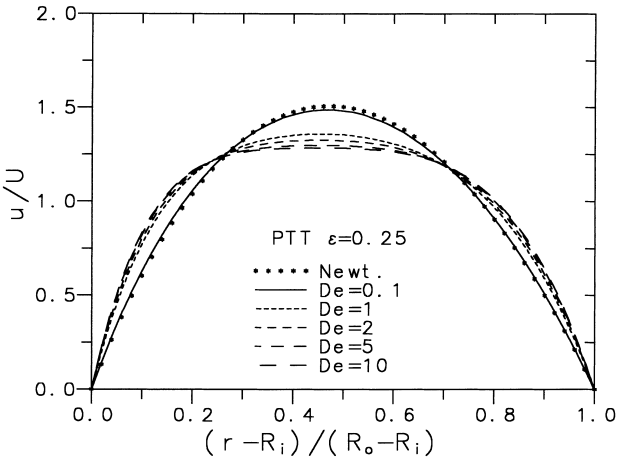

Fig. 3. Velocity profiles (u/U) for various De, as obtained from Eq. (12), at fixed values of $\epsilon=0.25$ and $k=0.5$.

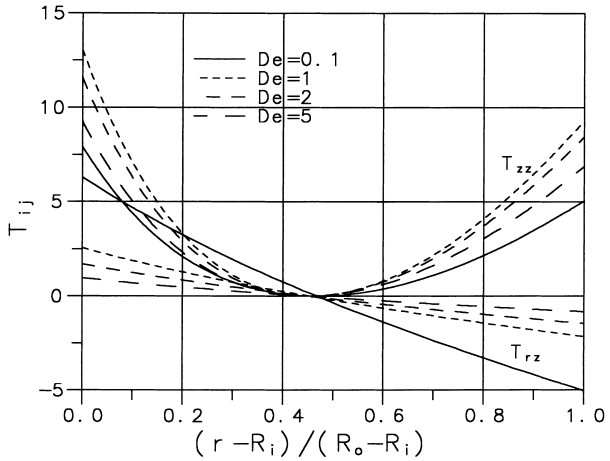

Fig. 4. Stress profiles ($T_{ij}=\tau_{ij}/(\eta U/\delta)$) for various De, as obtained from Eqs. (5) and (9), at fixed values of $\epsilon=0.25$ and $k=0.5$.

It is mentioned above that the coupling involved in the inverse problem of determining the pressure drop (that is, U_c) for a given flow rate (that is, U) can be effectively solved by iteration and this is quantified in Table 1 which gives the number of iterations required to achieve convergence up to 5-digits (relative error for both y_* and X below a tolerance of 10^{-5}) in some typical cases. Clearly, this simple iterative procedure converges fast and if 3-digits accuracy is acceptable, then 2 iterations only through Eqs. (16) and (23) are sufficient.

Some of the important features of the present solution for the velocity and stress variations are exemplified in Figs. 3 and 4, for varying De number at fixed $\epsilon=0.25$ and $k=0.5$. For low elasticity (De=0.1) the velocity variation in Fig. 3 differs little from the Newtonian case, but as De is increased the profiles become more flattened indicating the effect of shear-thinning. Such effect is absent from a purely elastic

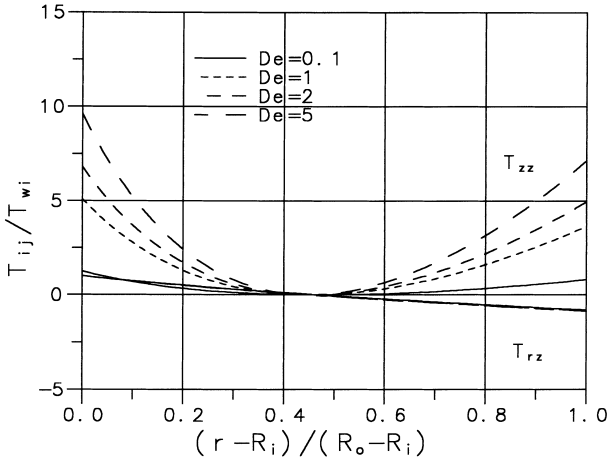

Fig. 5. Stress profiles scaled with the inner-wall shear stress value ($T_{ij}/T_{rz}(r=R_i)$).

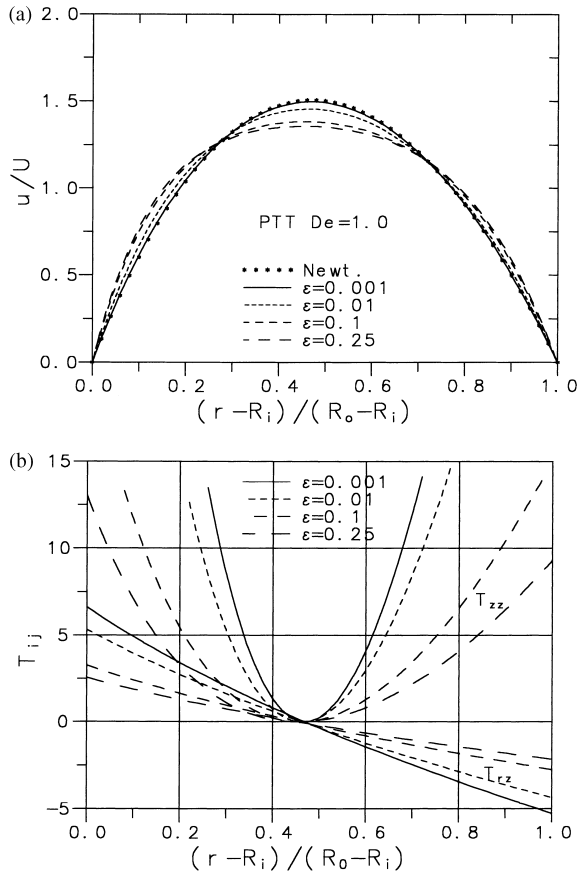

Fig. 6. Effect of the extensional parameter ε on the solution, at fixed De=1.0 and k=0.5: (a) velocity profiles; (b) stress profiles.

fluid model with infinite extensibility (that is, when ϵ=0 as for the UCM) but is one of the important features of the PTT model.

The variation of shear (T_{rz}, from Eq. (5)) and normal (T_{zz}, from Eq. (9)) stress components across the annular gap is given in Fig. 4 in terms of the normalised radial distance $(r-R_\mathrm{i})/\delta$. Although the variation of T_{rz} is monotonic with increased values of De, the same does not hold for T_{zz}. The normal stress increases when De goes from 0 to 1.0 and then decreases. Such behavioural pattern is due to shear-thinning at the wall and can be removed if the stresses are scaled with the inner wall shear stress value ($T_{wi}=T_{rz}$ at $r=R_\mathrm{i}$), as shown in Fig. 5: the different curves for T_{rz}/T_{wi} almost collapse onto a single curve as expected, and the normal stress variation is now monotonic with De.

An assessment of the effect of the elongation parameter of the model ϵ, on the solution field can be gained from Fig. 6. At fixed De=1 and k=0.5, Fig. 6a shows velocity profiles for ϵ=0.001, 0.01, 0.1 and 0.25, the range most likely to occur in practical applications. It is clear that as ϵ is reduced, the velocity profile becomes very close to the Newtonian curve and the solution is then independent of De, i.e. one gets the solution for the UCM model at all De. The axial normal stress (Fig. 6b) increases dramatically for small ϵ, reaching very high values near both the inner and outer cylinder walls. The variations for both T_{zz} and T_{rz} are monotonic with ϵ, at fixed De.

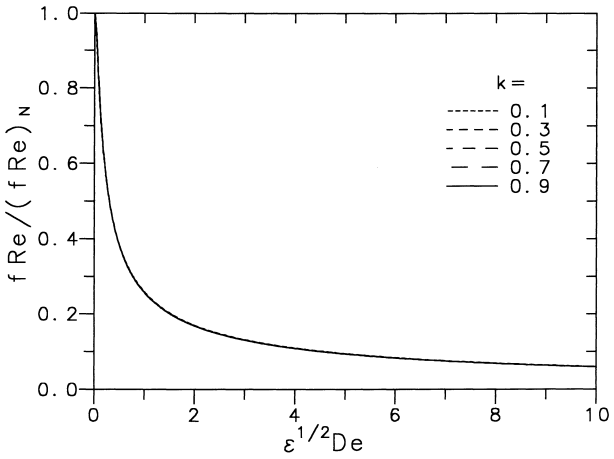

Fig. 7. Ratio of the viscoelastic to the Newtonian friction factor ($f\mathrm{Re}/f\mathrm{Re}_\mathrm{N}$) as a function of $\epsilon^{1/2}$ De, for various radius ratios k.

The effect of radius ratio on the velocity profile is similar to that observed with Newtonian fluids (Bird et al. [4]); as the annular gap increases in size the region of maximum velocity moves progressively towards the inner cylinder and the normalised maximum velocity $u_{\max}/U$ increases slightly.

In practical situations the parameter of most importance is the friction factor, which is better expressed in terms of $f\mathrm{Re}$, shown in the analysis to be proportional to the solution parameter X (Eq. (26)). Its variation with De is thus expected to follow trends similar to those in Fig. 1. In order to see how the viscoelastic results depart from the Newtonian, it is better to examine the ratio of $f\mathrm{Re}$ to the corresponding Newtonian values, $(f\mathrm{Re})_\mathrm{N}$ from Eq. (25). Fig. 7 shows a reduction in wall friction imparted by elasticity coupled with extensibility. The important finding from Fig. 7 is, however, that there is no influence of the radius ratio on the variation of the friction factor ratio ($f\mathrm{Re}/(f\mathrm{Re})_\mathrm{N}$) with elasticity, as measured by $\epsilon^{1/2}$ De — the collapse seen in the figure of all curves onto a single curve is perfect. This property could not be foreseen

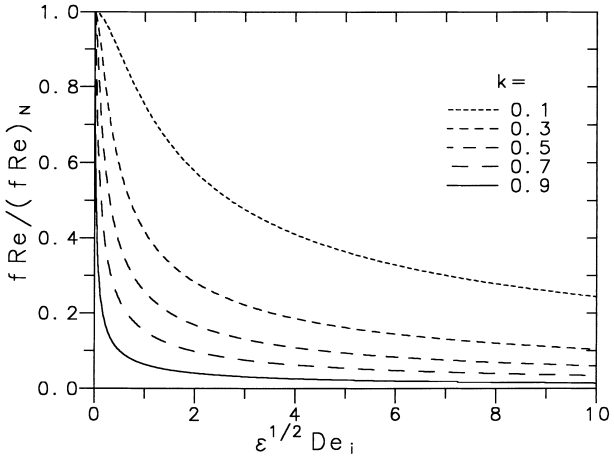

Fig. 8. Effect of a different scaling on the friction factor ratio ($\mathrm{De}_\mathrm{i} = \lambda U/R_\mathrm{i}$).

from the form of the solution which exhibits dependence on k in various terms (cf. Eqs. (20)–(23)). Indeed, it is interesting to plot the information in Fig. 7 but as a function of a differently-defined Deborah number, $De_i = \lambda U/R_i$. This is presented in Fig. 8 and, under this scaling, different curves are obtained for different k, hence demonstrating the lesser universality of a scaling based on taking R_i (or even R_o) as the length scale.

Acknowledgements

This work has been carried out while the second author was in a sabbatical leave supported by Fundação para Ciência e Tecnologia (FCT, Portugal) under grant FMRH/BSAB/68/99 which is here gratefully acknowledged.

References

[1] N. Phan-Thien, R.I. Tanner, A new constitutive equation derived from network theory, J. Non-Newtonian Fluid Mech. 2 (1977) 353–365.
[2] J.L. Kokini, C.F. Wang, H. Huang, S. Shrimanker, Constitutive models of foods, J. Text. Studies 26 (1995) 421–455.
[3] N.J. Alderman, D. Ram Babu, T.L. Hughes, G.C. Maitland, The rheological properties of water-based drilling muds, in: Proceedings of the 10th International Congress on Rheology, Sydney, 14–19 August 1988.
[4] R.B. Bird, W.E. Stewart, E.N. Lightfoot, Transport Phenomena, Wiley, New York, 1960.
[5] A.G. Fredrickson, R.B. Bird, Non-Newtonian flow in annuli, Ind. Eng. Chem. 50 (1958) 347–352.
[6] R.W. Hanks, K.M. Larsen, The flow of power-law non-Newtonian fluids in concentric annuli, Ind. Eng. Chem. Fundam. 18 (1979) 33–35.
[7] R.W. Hanks, The axial laminar flow of yield-pseudoplastic fluids in a concentric annulus, Ind. Eng. Chem. Proc. Des. Dev. 18 (1979) 488–493.
[8] R.B. Bird, R.C. Armstrong, O. Hassager, Dynamics of polymeric liquids: Fluid Mechanics, Vol. 1, Wiley, New York, 1977.
[9] C. Nouar, R. Devienne, M. Lebouche, Convection thermique pour l'écoulement de Couette avec debit axial; cas d'un fluide pseudoplastique, Int. J. Heat Mass Transfer 30 (1987) 639–647.
[10] M. Naimi, R. Devienne, M. Lebouche, Étude dynamique et thermique de l'écoulement de Couette–Taylor–Poiseuille; cas d'un fluide presentent un seuil d'écoulement, Int. J. Heat Mass Transfer 33 (1990) 381–391.
[11] M.P. Escudier, P.J. Oliveira, F.T. Pinho, S. Smith, Fully developed laminar flow of purely viscous non-Newtonian liquids through annuli, including the effects of eccentricity and inner-cylinder rotation, 2000, in preparation.
[12] J.G. Savins, G.C. Wallick, Viscosity profiles, dicharge rates, pressures, and torques for a rheologically complex fluid in helical flow, AIChE J. 12 (1966) 357–363.
[13] A.C. Dierckes, W.R. Schowalter, Helical flow of a non-Newtonian polyisobutelene solution, Ind. Eng. Chem. Fundam. 5 (1966) 263–271.
[14] L. Quinzani, R.C. Armstrong, R.A. Brown, Use of coupled birefringence and LDV studies of flow through a planar contraction to test constitutive equations for concentrated polymer solutions, J. Rheol. 39 (1995) 1201–1228.
[15] G.W.N. Peters, J.F.M. Schoonen, F.P.T. Baaijens, H.E.H. Meijer, On the performance of enhanced constitutive models for polymer melts in a cross-slot flow, J. Non-Newtonian Fluid Mech. 82 (1999) 387–427.
[16] S.A. White, D.G. Baird, Numerical simulation studies of the planar entry flow of polymer melts, J. Non-Newtonian Fluid Mech. 30 (1988) 47–71.
[17] F.P.T. Baaijens, Numerical analysis of start-up planar and axisymmetric contraction flows using multi-mode differential constitutive models, J. Non-Newtonian Fluid Mech. 48 (1993) 147–180.
[18] E.O.A. Carew, P. Townsend, M.F. Webster, A Taylor–Petrov–Galerkin algorithm for viscoelastic flow, J. Non-Newtonian Fluid Mech. 50 (1993) 253–287.
[19] J. Azaiez, R. Guenette, A. Aït-Kadi, Numerical simulation of viscoelastic flows through a planar contraction, J. Non-Newtonian Fluid Mech. 62 (1996) 253–277.
[20] A. Baloch, P. Townsend, M.F. Webster, On vortex development in viscoelastic expansion and contraction flows, J. Non-Newtonian Fluid Mech. 65 (1996) 133–149.